JOURNAL OF PROPULSION AND POWER
Vol. 26, No. 3, May–June 2010

Performance of Ammonium-Perchlorate-Based Composite Propellant Containing Nanoscale Aluminum

Matthew Stephens,* Thomas Sammet,† and Eric Petersen‡
Texas A&M University, College Station, Texas 77843
Rodolphe Carro§ and Steven Wolf‡
University of Central Florida, Orlando, Florida 32816
and
Christopher Smith¶
Space Launch Corporation, Irvine, California 92614

DOI: 10.2514/1.45148

Several composite propellant mixtures of hydroxyl-terminated polybutadiene, ammonium perchlorate, and aluminum were prepared with and without the addition of small percentages of nanoscale aluminum and tested in a strand burner at pressures up to 34.5 MPa. The effect of monomodal versus bimodal ammonium perchlorate particle size, coarse aluminum particle size, nano aluminum particle size, and coarse-to-fine ratios on burning rate and manufacturability were explored. A significant conclusion of the present study is that the addition of nanoscale aluminum does not always ensure an increase in the propellant's burning rate when produced using conventional methods. It was observed that over the range of mixtures and pressures explored, a bimodal oxidizer is required for the nanoscale aluminum to affect the burning rate, and that a monomodal oxidizer tended to nullify any influence of the nanoscale aluminum. In some cases, the addition of nanosized aluminum decreased the burning rate. The level of burning-rate increase or decrease depended on the bimodal or monomodal ammonium perchlorate particle sizes, the coarse aluminum particle size, and the pressure range.

Introduction

NANOPARTICLES are being considered in many aerospace propulsion applications, due in large part to their high surface-to-volume ratio and high reactivity. Nanoscale Al, sometimes referred to as ultrafine Al, is of special interest in applications ranging from hybrid rocket motor additives [1,2] to the main fuel source in Mars-based engines [3]. The topic of the present study is the use of nanoscale Al in hydroxyl-terminated polybutadiene and ammonium perchlorate (HTPB/AP)-based composite solid rocket propellants. Several studies indicate that a significant increase in burning rate is possible when some or all of the traditional micron-scale Al in metallized composite propellants is replaced by nanoparticles [4].

The activity of Al particle combustion in composite propellants has been a topic of focus for over four decades, starting with such works as those done by Crump et al. [5]. For example, particle size has been seen to have an impact on the acoustics within a solid rocket motor [6,7] and, as summarized by Waesche [8], aluminum particle size can play a role combustion instability. Also important to combustion instability is the characteristic of the leading-edge flame [9], which can be altered by the presence of aluminum particles. Through other past studies, it has been seen that the particle size can also have a large effect on the combustion temperature and flame structure of the Al particle [10].

Several recent works have produced strong theories explaining the mechanisms associated with nanoscale Al. These theories agree on one key aspect: nanoscale Al ignites and releases energy closer to the propellant burning surface than its micron-scale counterpart. Unless specially treated, all particles of Al have an oxide coating (Al_2O_3), which melts at 2047°C versus the 660°C melting temperature of Al. When the pure Al core is melted, it expands 6% in volume; one theory proposes that this expansion is not strong enough to break the Al_2O_3 coating on micron-sized particles but is sufficient enough to break the coating on Al nanoparticles. This ability allows the particle to crack the oxide coating earlier, thus burning closer to the surface. This process is best described in detail by Dokhan et al. [11]. Other works, such as Mullen and Brewster's [12], have shown that this Al_2O_3 cracking in micron-scale particles can cause significantly large Al agglomerations. It has also been suggested by Mench et al. [13] that another factor in the success of nanoscale Al is the enormous increase in Al-to-binder contact area due to the high surface-to-volume ratio of the Al nanoparticles. This increase in surface area leads to an increase in heat transfer (as well as other factors), because the nanoparticles heat up to their melting temperature much more quickly than micron-scale particles.

By using a high-speed camera (1000 frames/second), Dokhan et al. [14] were able to view an intense brightness on the burning surface of the propellant that is only existent with the use of nanoscale Al. This photographic evidence strongly supports the theory regarding Al ignition near the burning surface. In their series of tests, nanoscale Al was shown to increase the burning rate over twofold when used as the entire Al content. The effect of the oxidizer on the burning of nanoscale Al was also explored. In another study, Dokhan et al. [15] collected the exhaust particles of the propellant and observed in the experiment that when the oxidizer contains 82.5 μm AP particles, there is a severe decrease in the quantity of large exhaust particles. This reduction may indicate a more efficient burning of the larger Al or a decline of Al agglomeration. At Valcartier in Canada, Lessard et al. [16] have shown drastic increases in burning rates by introducing nanoscale Al at a maximum of 20% of the total Al content. They were also able to produce a plateau effect in

Presented as Paper 4470 at the 41st AIAA/ASME/SAE/ASEE Joint Propulsion Conference and Exhibit, Tucson, AZ, 10–13 July 2005; received 27 April 2009; revision received 12 January 2010; accepted for publication 14 January 2010.

*Research Assistant, Department of Mechanical Engineering. Student Member AIAA.
†Research Assistant Engineer, Department of Mechanical Engineering. Member AIAA.
‡Associate Professor, Department of Mechanical Engineering. Senior Member AIAA.
§Research Assistant, Mechanical, Materials, and Aerospace Engineering. Student Member AIAA.
¶Research Engineer; currently Engineer, Aerojet, Sacramento, CA.

the 10.34–15.17 MPa pressure range with a propellant containing nanoscale Al. As first observed by Dokhan et al. [17], nanoscale Al can lead to enhanced heat feedback near the surface, due to increased radiation heat transfer.

There are also some drawbacks associated with nanoscale Al particles. These include a higher oxide content, a decrease in manufacturability, and an increase in cost when compared with conventional Al particles [17]. Another drawback is the decreased acoustic damping effect of Al nanoparticles, as shown by Blomshield et al. [18], which is most likely a product of the difference in exhaust particle sizes. However, Dokhan et al. [17] proposed an answer to the cost and manufacturing issues by only substituting a small fraction of the micron-scale Al in a propellant formulation with nanoparticles; this practice has also been done in other nanoscale Al propellant and thermite studies [16,19].

One goal of the present study was to explore the feasibility of producing HTPB/AP-based propellants containing nanoscale Al in the traditional batch mixer commonly used in large-scale production facilities. Another goal was to further explore the effects of monomodal and bimodal oxidizer, particle size of the oxidizer, and micron-scale Al particle size on the burning rate of mixtures containing Al nanoparticles. Details on the experimental approach and the mixtures investigated are provided first, followed by the results of high-pressure strand-burning experiments. Empirical analyses performed on the burning-rate data are provided and discussed.

Experiment

A series of experiments was performed to explore the effect of nanoscale Al on various composite propellant formulations. Nineteen HTPB/AP/Al formulas were studied; each formula contained a solids loading content of 88% by mass, with the Al content being 20% of the total mass in all cases. The formulas are best divided into three categories, depending on the coarse oxidizer particle size (200 or 400 μm), the coarse Al particle size (3 or 36 μm), and whether a monomodal or bimodal oxidizer size distribution was used.

The binder used in these propellants consisted of *R*-45M HTPB and Papi-94 (Dow Chemical) as a diphenylmethane diisocyanate curative, both from Aerocon Systems. The oxidizer used for this study was ammonium perchlorate (AP) and was procured from Skylighter, Inc. The micron-scale Al used was German black flake, and iron oxide (Fe_2O_3), 44 μm, was used as a burning-rate modifier, both from Firefox Enterprises. The nanoparticle Al used was supplied by Technanogy. The baseline percentages by mass were 10.56% HTPB, 20% Al, 0.5% Fe_2O_3, 67.5% AP, and 1.44% MDI. Propellants from formulas 10 through 19 (Table 1) included 0.2% Tepanol by mass (plasticizer) and less than 0.1% silicone oil (defoaming agent). These ingredients were added as processing aids and did not alter burning performance; this result was confirmed in a propellant test not included herein.

Nine different propellant mixtures were studied under the first set of formulas: mixtures 1–9 in Table 1. Each was based on 200 μm monomodal oxidizer and 3 μm Al. Mixtures 1 through 3 were all baseline compositions used for repeatability testing, and the other three incorporated nanoscale Al; their formulas can be found in Table 1. Formulas 4 through 9 all included nanoscale Al as a percentage substitute of the baseline Al level. This substitution is presented as a bimodal Al totaling the same 20% content by mass of the total mixture and now defining the 3 μm Al as the coarse Al (cAl) and the nanoscale Al as the fine Al (fAl). This size of cAl is often referred to as fAl, but for this study the coarse and fine prefixes are used to classify the two separate sizes in a bimodal mixture and not a preestablished size category. The formulas used relatively small coarse-to-fine (c/f) Al ratios due to the poor physical strength and manufacturability issues associated with higher nanoscale Al loadings. Similar effects were described by Shalom et al. [20]. Three distinct sizes of Al nanoparticles were used at varying c/f ratios: 201, 134, and 47 nm.

The second set of formulas (mixtures 10–12 and 17) investigated the use of a bimodal oxidizer, again using the prefixes c and f for coarse and fine designations of the AP distribution. The cAP was stock 200 μm, and the fAP was 82.5 μm. The fAP was processed in the authors' laboratory using a ball mill and test sieves. The top sieve was no. 170 mesh, 90 μm, and the bottom was no. 200 mesh, 75 μm, which made for a nominal size of 82.5 $\pm$ 7.5 μm. Table 1 shows the four formulas in the second series of tests (mixtures 10–12 and 17). The first three mixtures of this series (10–12 in Table 1) explored bimodal AP at different c/f ratios within the baseline coarse Al size (3 μm). Mixture 17 incorporated Al nanoparticles with bimodal AP.

The third series of formulas investigated the use of larger Al and oxidizer coarse particles. In this series, the 3 μm Al was replaced with 36 μm Al (mixtures 14, 16, 18, and 19 in Table 1), and the 200 μm AP was replaced with 400 μm AP (mixtures 13 and 15). This approach was also coupled with both the bimodal AP approach and the nanoscale Al investigation in mixtures 13, 16, 18, and 19. Organized details of these mixtures are presented in Table 1.

All propellant mixtures were produced in 500 g batches to ensure thorough mixing and to increase the ratio mix accuracy. A quart-sized, high-shear mixer was used to mix each batch. The propellant was pressed into Teflon tubes (0.64 cm o.d., 0.48 cm i.d., and roughly 2.54 cm long) and cured at 55°C for at least 48 h. Repeatability of the mixing procedure was verified in previous experiments, and a sample comparison for the baseline mixture is provided in the Results section.

Samples from all 19 propellants were tested in a high-pressure strand bomb at pressures ranging from 3.4 to 34.5 MPa; this test hardware is similar in nature to a Crawford strand bomb [21]. Each sample was stripped of its Teflon tube and coated with HTPB as an

Table 1 Propellant compositions for the present study

Mixture	c/f AL	cAl size, μm	fAl size, nm	c/f AP	cAP size, μm	fAP size, μm
Baseline (1–3)	100/00	3	——	100/00	200	——
4	95/5	3	201	100/00	200	——
5	85/15	3	201	100/00	200	——
6	85/15	3	134	100/00	200	——
7	85/15	3	47	100/00	200	——
8	70/30	3	201	100/00	200	——
9	95/5	3	134	100/00	200	——
10	100/00	3	——	80/20	200	82.5
11	100/00	3	——	60/40	200	82.5
12	100/00	3	——	40/60	200	82.5
13	100/00	3	——	80/20	400	82.5
14	100/00	36	——	100/00	200	——
15	100/00	3	——	100/00	400	——
16	100/00	36	——	80/20	200	82.5
17	85/15	3	134	80/20	200	82.5
18	85/15	36	134	80/20	200	82.5
19	85/15	36	134	100/00	200	——

inhibitor on all sides except the initiation end. After being placed in the strand bomb, the samples were ignited by running a high voltage across a thin-gauge Nichrome wire in contact with the uninhibited end. The computer data acquisition system (Gage Applied Sciences) captured pressure traces and light emission, while a streaming-video feed captured live footage of each burn. The burning rate was determined by dividing the sample's length by the burning time deciphered from the pressure trace. Pressure increases inside the chamber averaged no more than 10% of the initial pressure, and the burning rates were assigned to the average test pressure. The light emission and video footage were used to confirm burning times and assess the quality of a given burn. Further details of the strand testing procedure and facility are given by Carro et al. [22].

Since it has been shown by other investigators that tiny voids in the finished propellant can cause intermittent and (usually) greatly accelerated burning, much care was taken to watch for such effects and to eliminate their presence by perfecting the mixing technique. Such voids are more likely to occur when using significant levels of nanoscale fuel particles. For example, the mechanical mixing process mentioned above used a vacuum system that was always on while mechanically mixing the propellants in Table 1. Voids can sometimes be detected while burning samples, where the evidence is manifested in an oscillatory pressure trace and/or in visible flashing. Early in the present investigation, while perfecting the techniques used to manufacture the mixtures in Table 1, the authors occasionally made bad batches that did have microscopic voids that resulted in sporadic and highly accelerated burning. Hence, the authors knew what to look for when conducting the good experiments shown herein.

Percent theoretical density was also monitored for each mixture, the results of which are displayed in Table 2. As is shown in the Results section, the experiments presented herein were very repeatable (see Results section), in contrast to what would otherwise be the case if voids were a problem. All data presented herein were free of any evidence of accelerated burning due to small voids.

Results

As shown in Table 1, the first three mixtures were all composed of the baseline formula (monomodal 200 μm AP and 3 μm Al). The burning-rate data from these mixtures are shown in Fig. 1. The results for mixtures 1 through 3 are all within a short margin of each other and are well characterized by the burning-rate curve shown. Figure 1 is also a good example of the experimental repeatability and overall burning-rate uncertainty, represented by the variation of the data from the average trend and summarized by the error bars shown. The uncertainty for all data herein is estimated to be ± 0.12 cm/s, based on the statistical variation in the data points and the precision of the burning-rate measurement from the pressure and emission data. Only representative error bars are shown in Fig. 1 (and in all figures) for convenience and clarity, rather than putting them on every point.

Table 2 Empirical analysis, percent theoretical density, and physical testing results for the baseline and experimental propellant mixtures, with burning rate given as $r_b = aP^n$ in cm/s

Mixture	a	n	R^2	$\%\rho_{th}$	Strength
Baseline	0.3686	0.63	0.98	0.98	Good
4	0.3847	0.63	0.97	0.96	Good
5	0.4465	0.50	0.98	0.94	Fair
6	0.3765	0.59	0.99	0.99	Poor
7	0.4044	0.59	0.94	0.94	Poor
8	0.4074	0.56	0.98	0.94	Fair
9	0.3624	0.61	0.97	0.92	Good
10	0.3230	0.75	0.97	0.95	Good
11	0.2870	0.90	0.98	0.98	Good
12	0.2850	1.08	0.98	0.94	Good
13	0.3178	0.57	0.98	0.99	Good
14	0.7714	0.33	0.98	0.97	Good
15	0.1999	0.76	0.98	0.99	Poor
16	1.4687	0.13	0.89	0.89	Fair
17	0.7176	0.37	0.97	0.92	Poor
18	0.1303	1.12	0.99	0.84	Poor
19	0.7471	0.30	0.99	0.87	Fair

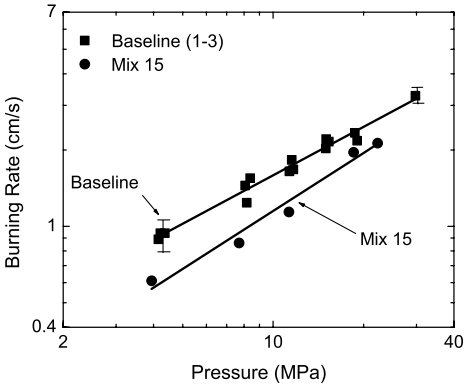

Fig. 1 Burning-rate curves of the baseline propellant (mixtures 1–3, 200 μm AP and 3 μm Al) and a similar propellant with a coarser oxidizer (mixture 15, 400 μm AP and 3 μm Al). Typical error bars are shown on the baseline mixture results.

Mixture 15 is presented on the same plot with the baseline mixtures since it shares the baseline's formula with the exception of using 400 μm AP. By using the larger oxidizer particle size, the magnitude of the burning-rate curve decreased, whereas the slope increased, indicating that the smaller oxidizer produces a less-pressure-sensitive propellant when compared with the coarser-AP mixture. The empirical data for the burning-rate curves can be found in Table 2. For the 0.48-cm-diam samples, the mixtures with the 400 μm AP typically had 10–12 AP particles across the diameter, which was deemed sufficient to minimize any potential edge effects. No comparisons were made on the effect of sample diameter for the larger-AP mixtures when compared with the 200-mm-AP mixtures, although no abnormal burning results were seen. The burning-rate trend for mixture 15 when compared with the baseline mixture follows the trend expected from the literature for similar-sized monomodal-AP-based composite propellants.

As seen in Fig. 1, and in all other graphs, the burning rates are plotted versus pressure on a log–log scale illustrating a linear relationship between burning rate and pressure. Another feature common in all plots is that any mixture containing nanoscale Al is represented by hollow data points, whereas all others use solid data points. The burning-rate curves use the logarithmic form of

$$r_b = aP^n$$

where r_b is the burning rate (in cm/s), a is the leading coefficient, P is the pressure (in MPa), and n is defined as the pressure exponent. The curve-fit regression parameter R^2 is also listed in Table 2. The pressure exponent directly corresponds to a burning-rate curve's slope: a high slope produces a large n value, whereas a low slope produces a small n value. The percent theoretical density $\%\rho_{th}$ is defined as the measured density over the theoretical density and is presented in Table 2, as mentioned above. The measured density is an average of the density of individual test samples from a batch.

The next six propellant mixtures incorporated nanoscale Al directly into the baseline formula (i.e., 4–9 in Table 1). The burning-rate data from the propellants using 201 nm fAl (mixtures 4, 5, and 8) are presented in Fig. 2. Here, it is apparent that there is not much difference between the three mixtures; all three closely match one another and have nearly the same spread of data points. Figure 3 contains the other three propellants that incorporated Al nanoparticles directly into the baseline formula (mixtures 6, 7, and 9). These mixtures used 134 or 47 nm fAl integrated into the baseline formula at various percentages of the total Al content. These propellants show even more indifference, all sharing nearly the same burning-rate curve.

Physical testing was conducted that rated propellants on their material strengths based upon hand-manipulating samples and

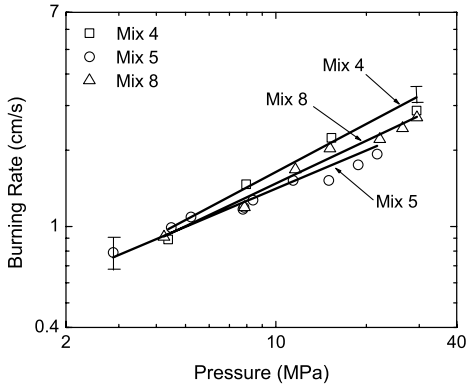

Fig. 2 Burning-rate curves of propellants containing 3 μm cAl and 201 nm fAl at various c/f ratios (95/5 in mixture 04, 85/15 in mixture 05, and 70/30 in mixture 08); all have monomodal 200 μm AP. Typical error bars are shown on the mixture 4 results.

qualitatively judging them relative to the baseline propellant; therefore, the baseline was rated as having strong properties. Analysis of mixtures 6 through 9 demonstrated that higher concentrations of fAl reduced physical strength and caused the propellant to become susceptible to crumbling; reduced sizes of fAl further weakened the propellant. The physical-strength results along with the empirical analysis of mixtures 4 through 9 (and the baseline) are also located in Table 2.

A summary comparison amongst all six propellants' burning curves and the baseline can be seen in Fig. 4. Here, it is clear how insignificantly the burning rate was affected. The only real difference observed was that the mixtures with nanoscale Al tended to have slightly lower reduced magnitudes. Hence, the expected burning-rate increase due to the addition of the nanoscale Al was not observed.

The next five propellants, mixtures 10 through 13 and 17, all incorporated a bimodal oxidizer and the monomodal Al (3 μm) from the baseline formula. Figure 5 shows the burning-rate data and curves of these propellants compared against each other. Mixtures 10 through 12 demonstrated that larger fAP percentages increased both the magnitude and slope of the burning curve, as expected. The larger cAP (400 μm) in the bimodal-AP mixture 13 drastically reduced both the pressure exponent and magnitude. Referring to Table 2, it is apparent that mixture 13 highly resembles the baseline values. Mixture 17, which mimicked mixture 10's formula (80/20 c/f AP) with the addition of nanoscale Al (134 nm) at 15% of the total Al loading, exhibited a drastically reduced pressure exponent when compared with mixture 10. This result meant that at low pressures, the nanoscale Al increased the burning rate but consequently decreased the burning rate at higher pressures, above approximately 6.9 MPa.

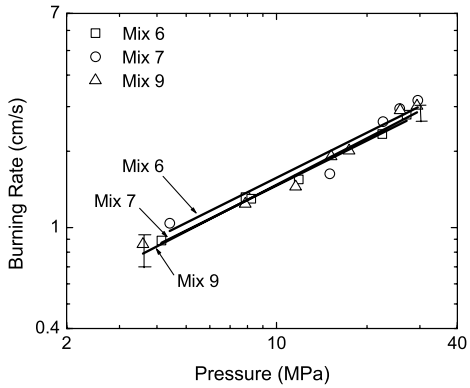

Fig. 3 Burning-rate curves of propellants containing 3 μm cAl and 134 nm fAl at various c/f ratios ((95/5 in mixture 09 and 85/15 in mixture 06) or 47 nm fAl at a c/f ratio of 85/15 (mixture 07); all have monomodal 200 μm AP. Representative error bars are shown for mixture 7.

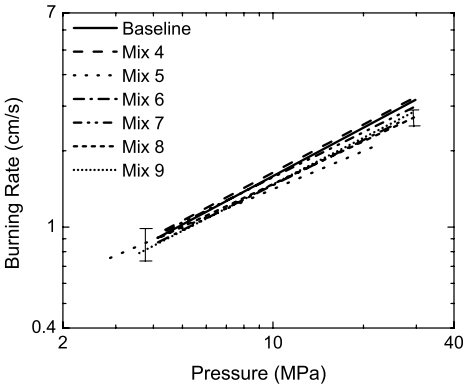

Fig. 4 Comparison between the baseline and the propellants with only the addition of nanoscale Al in place of a portion of baseline's micron-scale Al. Representative error bars are shown at pressure extrema.

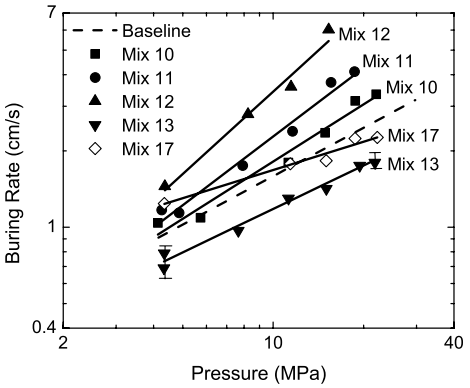

Fig. 5 Burning-rate curves of bimodal oxidizer propellants at various c/f ratios (80/20 in mixture 10, 60/40 in mixture 11, and 40/60 in mixture 12). Mixture 13 used 400 μm cAP in a c/f AP ratio of 80/20. Mixture 17 had an AP c/f ratio of 80/20 and an Al c/f ratio of 85/15 using 134 nm fAl. Typical error bars are shown on mixture 13 as a guide.

Figure 6 shows the results of replacing the 3 μm Al with 36 μm Al. Mixture 14 represents a baseline formula with the use of the 36 μm Al, and mixture 19 incorporated a small percentage of nanoscale Al at a c/f Al ratio of 85/15 in addition to the new, larger, cAl size. The reduced slope of mixture 14 compared with the baseline indicates that the larger-sized Al particle helped stabilize the propellant's pressure sensitivity. For this larger cAl particle size, nanoscale Al reduced the burning rate by only a very noticeable margin, indicating again that it appeared to have very little impact on the burning rate.

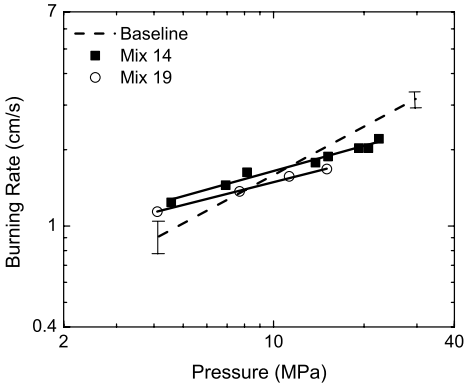

Fig. 6 Burning-rate curves of propellants that contained monomodal 36 μm Al, mixture 14, and also combined with nanoscale Al, mixture 19, at a c/f Al ratio of 85/15. Both have monomodal, 200 μm AP. Representative error bars are shown on the baseline curve as a guide.

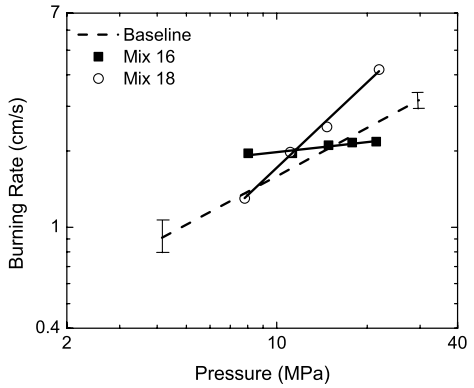

Fig. 7 Burning-rate curves of mixture 16 (monomodal 36 μm Al) and mixture 18 (85/15 c/f Al with 134 nm fAl); both having 80/20 c/f AP with 200 μm cAP. Typical error bars are shown on the baseline curve as a guide.

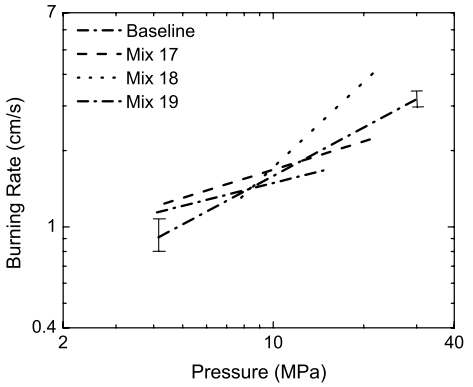

Fig. 8 Summary comparison of the baseline burning-rate curve and the propellants that contained nanoscale Al and: a bimodal oxidizer (mixture 17), 36 μm Al (mixture 19), or both (mixture 18). Representative error bars are shown on the baseline curve as a guide.

Propellants that incorporated both the bimodal oxidizer (80/20 c/f AP ratio) and the larger Al particles (36 μm) are shown in Fig. 7. Whereas the monomodal Al propellant (mixture 16) drastically reduced the pressure exponent to the lowest value seen in the present work, the bimodal Al (85/15 c/f Al ratio) propellant (mixture 18) that incorporated 134 nm fAl exhibited the highest pressure exponent [although no evidence of accelerated burning due to potential voids was observed for this mixture, it did have the lowest theoretical density (Table 2)]. Because of the increased slope, Al nanoparticles created much lower burning rates at low pressures (less than 10.34 MPa), but drastically increased burning rates at higher pressures.

Mixtures 10 through 19 are described in Table 2 by their empirical values, percent theoretical density, and qualitative physical strengths. Referring to the R^2 values in Table 2, it is clear how well these propellants are characterized by the empirical data. The high-percent theoretical densities in Table 2 (except possibly mixture 18) also show that the propellants were well compacted, with reduced chances for voids or defects.

Discussion

A significant observation of the present study is that the simple substitution of nanoscale Al in place of a portion of the micron-scale Al in a composite solid propellant does not automatically lead to an increase in the propellant's burning rate. In some cases, the addition of Al nanoparticles can even decrease the burning rate. The impact of nanoscale Al addition on the burning rate of a HTPB/AP-based propellant, when mixed using conventional mechanical methods, appears to depend on the AP size distribution, the size of the coarse Al particles, and the pressure range. For example, from mixtures 4 through 9 with monomodal AP and 3 μm cAl, adding nanoscale Al directly to the baseline's fundamental formula had a negligible effect, slightly decreasing the burning rate in most cases. In the subsequent experiments described above, it was found that a bimodal oxidizer was needed to properly ignite and burn the nanoscale Al. This result may be due in large part to the leading-edge-flame (LEF) phenomenon that characterizes the burning behavior of AP particles, attributed to Price [23]. The LEF's role in Al ignition has been well explained and modeled by Srinivas and Chakravarthy [24]. As described by Dokhan et al. [14], the fAP creates a canopy flame (a merged, premixed flame) over the HTPB/fAP/Al matrix on the propellant's burning surface. This canopy flame is responsible for the oxidation, and the LEF generated by the cAP is responsible for the heat required for Al particle ignition.

Without the use of nanoscale Al, the propellant's slopes were shown to increase upon increased levels of fAP. This same trend was demonstrated by a set of experiments done by Lee et al. [25]. Also, this fine-AP effect supports the prediction of Dokhan et al. [14] that 82.5 μm fAP particles generate LEF's at higher pressures. The effect of monomodal, 400 μm AP in reducing the burning rate is supported by the explanations posed in the work done by Lee et al. [25]. With large sizes of AP, only the outer perimeter of the particle effectively contributes to a strong HTPB/AP flame. The inner surface produces a weaker AP flame that does not provide considerable heat transfer back to the propellant's surface to increase the burning rate. Out of the three c/f ratios explored using 200 μm AP, the 80/20 ratio showed the least increase in slope when compared with the increase in burning rate.

The replacement of 3 μm Al with the larger, 36 μm Al in mixture 14 showed a reduction in the burning rate as compared with the baseline mixture at higher pressures. This decrease in r_b could signify that larger Al particles ignite further away from the propellant surface and do not contribute greatly to the heat feedback. It was also seen that the burning-rate slope, as seen in Table 2, was severely lower for mixture 14 and thus more stable than the baseline. Dokhan et al. [14] also show similar findings.

Mixture 17 used the bimodal findings and incorporated nanoscale Al at a c/f ratio of 85/15, with 3 μm cAl. This propellant is compared with the baseline and other nanoscale-Al-containing propellants in Fig. 8. It is apparent that at lower pressures the nanoscale Al produced nearly a factor-of-two increase in burning rate, verifying that the use of a bimodal oxidizer is needed to increase the burning rate. However, the reduced slope dictates lower burning rates at higher pressures when compared with the baseline. As shown in Fig. 5, when compared with the same bimodal-AP mixture with only cAl (mixture 10), the nano-Al-containing mixture 17 also produced an increase in burning rate only at lower pressures.

At higher pressures, mixture 19, which replaced 3 μm Al with the larger (36 μm) Al, showed a slight reduction in the burning rate as compared with the baseline mixture (Fig. 8). The combination of both the bimodal oxidizer and the 36 μm Al (mixture 18) supports all of the aforementioned conclusions. Here, since the nanoscale Al is ignited by the bimodal oxidizer, it is able to increase the energy enough near the burning surface to increase the burning rate. Since the increase in the burning rate is marginally small at first, it is likely that the nanoscale Al burning region does not produce enough heat to foster larger 36 μm Al particle ignition at low pressures. Recall from Fig. 7 that when compared with the same bimodal-AP distribution without nano Al, mixture 18 showed a dramatic increase in burning rate for pressures above approximately 11.72 MPa (albeit with a large pressure exponent). This result indicates that cAl ignition may increase with proximity to the burning surface after this point.

Conclusions

In this study, 19 propellants were formulated and mixed with varying characteristics to better understand the criteria needed for Al nanoparticles to be beneficial. Three propellants followed a baseline formula with monomodal AP (200 μm) and a typical loading of 3 μm Al to illustrate facility and procedure repeatability. The next six mixtures attempted to incorporate nanoscale Al in the simplest

manner, by directly adding it to the baseline formula. This series was done with three sizes of nanoscale Al (201, 134, and 47 nm) at three different ratios. There was no significant alteration of the burning rate by this method, although it was evident that the addition of nanoscale Al actually reduced the burning rate slightly in most cases.

A bimodal oxidizer was used in the next three propellants. These mixtures demonstrated that a higher fraction of fAP increases the burning slope. Two propellants mimicked the baseline again, one with a larger oxidizer size (400 μm) and the other with a larger Al size (36 μm). Both of these proved to reduce the burning rate noticeably, as seen by previous investigators. The Al size increase greatly decreased the slope as well, while the oxidizer size increase only slightly affected the slope. Another two mixtures combined these alterations with a bimodal oxidizer that reinforced the aforementioned conclusions.

Three final mixtures were made that incorporated the nanoscale Al into a bimodal oxidizer formula, an increased cAl-sized formula, and a formula including both alterations (larger cAl and bimodal AP). The addition of nanoscale Al to the mixture using the increased cAl size actually reduced the burning rate. Addition of nanoscale Al to the other two mixtures using a bimodal oxidizer successfully increased their burning rates over limited ranges of pressure. One significant conclusion is that a bimodal oxidizer seems to be required to achieve an increase in burning rate using nanoscale Al. This behavior should be explored further in future studies. The level of burning-rate enhancement also depends on the pressure and the size of the cAl particles to which the nano Al is added.

Acknowledgments

Partial funding for this work and some of the equipment used were supplied by the Space Launch Cooperation, Irvine, California. Additional funding was provided, in part, by the National Science Foundation, Research Experiences for Teachers grant number EEC-0401926, and the University of Central Florida (UCF). These experiments were originally performed when all of the primary authors were at UCF. Additional help in the laboratory over the course of these experiments was provided by Ray Simeone, Jennifer Small, Andreiev Powell, Thanh Hoang, and Alexander LePage; the authors are grateful for their efforts.

References

[1] Evans, B., Favorito, N. A., Boyer, E., Risha, G. A., Wehrman, R. B., and Kuo, K. K., "Characterization of Nano-Sized Energetic Particle Enhancement of Solid-Fuel Burning Rates in an X-Ray Transparent Hybrid Rocket Engine," AIAA Paper 2004-3821, July 2004.

[2] Risha, G. A., Boyer, E., Wehrman, R. B., and Kuo, K. K., "Performance Comparison of HTPB-Based Solid Fuels Containing Nano-Sized Energetic Powder in a Cylindrical Hybrid Rocket Motor." AIAA Paper 2002-3576, July 2002.

[3] Laritchev, M. N., Jigatch, A. N., Leipunsky, I. O., Kuskov, M. L., and Pshechenkov, P. A., "Aluminum Nanoparticles as the Energy Source for Mars Conditions (Multi-Sample Return Mission, Power Plants). Part 2," AIAA Paper 2003-4443, July 2003.

[4] De Luca, L. T., Galfetti, L., Severini, F., Meda, L., Marra, G., Vorozhtsov, A. B., Sedoi, V. S., and Babuk, V. A., "Burning of Nano-Aluminized Composite Rocket Propellants," *Combustion, Explosion and Shock Waves*, Vol. 41, No. 6, 2005, pp. 680–692. doi:10.1007/s10573-005-0080-5

[5] Crump, J. E., Prentice, J. L., and Kraeutle, K. J., "Role of the Scanning Electron Microscope in the Study of Solid Rocket Propellant Combustion: Part II. Behavior of Metal Additives." *Combustion Science and Technology*, Vol. 1, 1969, pp. 205–223. doi:10.1080/00102206908952201

[6] Dobbins, R. A., and Temkin, S., "Measurements of Particulate Acoustic Attenuation," *AIAA Journal*, Vol. 2, No. 6, 1964, pp. 1106–1111. doi:10.2514/3.2483

[7] Dobbins, R. A., and Temkin, S., "Propagation of Sound in a Gas-Particle Mixture and Acoustic Combustion Instability," *AIAA Journal*, Vol. 5, No. 12, 1967, pp. 2182–2186. doi:10.2514/3.4406

[8] Waesche, R. H. W., "Mechanisms and Methods of Suppression of Combustion Instability by Metallic Additives," *Journal of Propulsion and Power*, Vol. 15, No. 6, 1999, pp. 919–922. doi:10.2514/2.5517

[9] Beiter, C. A., and Price, E. W., "Leading-Edge Flame Detachment: Effect on Pressure-Coupled Combustion Response," *Journal of Propulsion and Power*, Vol. 14, No. 2, 1998, pp. 160–165. doi:10.2514/2.5281

[10] Bazyn, T., Glumac, N., and Krier, H., "The Combustion Characteristics of 10-Micron Aluminum Particles at Elevated Termperature and Pressure," AIAA Paper 2005-4466, July 2005.

[11] Dokhan, A., Price, E. W., Seitzman, J. M., and Sigman, R. K., "The Ignition of Ultra-Fine Aluminum in Ammonium Perchlorate Solid Propellant Flames," AIAA Paper 2003-4810, July 2003.

[12] Mullen, J. C., and Brewster, M. Q., "Investigation of Aluminum Agglomeration in AP/HTPB Composite Propellants," AIAA Paper 2006-280, Jan. 2006.

[13] Mench, M. M., Yeh, C. L., and Kuo, K. K., "Propellant Burning Rate Enhancement and Thermal Behavior of Ultra-Fine Aluminum Powders (Alex)," *Energetic Materials Production, Processing and Characterization—Proceedings of the 29th Annual Conference of ICT*, DWS Werbeagentur and Verlag GmbH, Karlsruhe, Germany, 1998, pp. 30-1–30-15.

[14] Dokhan, A., Price, E. W., Seitzman, J. M., and Sigman, R. K., "Combustion Mechanisms of Bimodal and Ultra-Fine Aluminum in AP Solid Propellant," AIAA Paper 2002-4173, July 2002.

[15] Dokhan, A., Price, E. W., Seitzman, J. M., and Sigman, R. K., "The Effects of Al Particle Size on the Burning Rate and Residual Oxide in Aluminized Propellants," AIAA Paper 2001-3581, July 2001.

[16] Lessard, P., Beaupré, F., and Brousseau, P., "Burn Rate Studies of Composite Propellants Containing Ultra-Fine Metals," *Energetic Materials Production, Processing and Characterization—Proceedings of the 29th Annual Conference of ICT*, DWS Werbeagentur and Verlag GmbH, Karlsruhe, Germany, 1998, pp. 88-1–88-13.

[17] Dokhan, A., Price, E. W., Seitzman, J. M., and Sigman, R. K., "The Effects of Bimodal Aluminum with Ultrafine Aluminum on the Burning Rates of Solid Propellants," *Proceedings of the Combustion Institute*, Vol. 29, 2002, pp. 2939–2945. doi:10.1016/S1540-7489(02)80359-5

[18] Blomshield, F. S., Nguyen, S., Matheke, H., Atwood, A., and Bui, T., "Acoustic Particle Damping of Propellants Containing Ultra-Fine Aluminum," AIAA Paper 2004-3722, July 2004.

[19] Moore, K., Pantoya, M. L., and Son, S. F., "Combustion Behaviors Resulting From Bimodal Aluminum Size Distributions," AIAA Paper 2005-3605, July 2005.

[20] Shalom, A., Aped, H., Kivity, M., and Horowitz, D., "The Effect of Nanosized Aluminum on Composite Propellant Properties," AIAA Paper 2005-3604, July 2005.

[21] Crawford, B. L., Huggett, C., Daniels, F., and Wilfong, R. E., "Direct Determination of Burning Rates of Propellant Powders," *Analytical Chemistry*, Vol. 19, No. 9, 1947, pp. 630–633. doi:10.1021/ac60009a004

[22] Carro, R., Arvanetes, J., Powell, A., Stephens, M. A., Petersen, E. L., and Smith, C., "High-Pressure Testing of Composite Solid Propellant Mixtures: Burner Facility Characterization," AIAA Paper 2005-3617, July 2005.

[23] Price, E. W., "Effect of Multidimensional Flamelets in Composite Propellant Combustion," *Journal of Propulsion and Power*, Vol. 11, No. 4, 1995, pp. 717–728. doi:10.2514/3.23897

[24] Srinivas, V., and Chakravarthy, S. R., "Computer Model of Aluminum Agglomeration on the Burning Surface of a Composite Solid Propellant," AIAA Paper 2005-743, Jan. 2005.

[25] Lee, S. T., Hong, S. W., and Yoo, K. H., "Experimental Studies Relating to the Combustion Microstructure in Heterogeneous Propellants," AIAA Paper 93-1753, June 1993.

S. Son
Associate Editor